Chapter 3

Synthesis and characterization of thermo responsive poly (MMA-co-VCL) copolymeric nanoparticles for encapsulation and in-vitro release of anticancer agent "etoposide"

Contents

3.1 Introduction

Considerable research attention has been focused recently on materials that change their structure and properties in response to external chemical and / or physical stimuli[1-10]. These materials are called "intelligent" or "smart" materials. They are also named as "stimuli-responsive" or "Intelligent" polymers. "Intelligent" polymers, with a balance of hydrophilic and hydrophobic groups, can respond to environmental stimuli, such as pH, temperature, and ions by changing their properties like volume and surface energy[11]. These changes are apparent at the macroscopic level as precipitate formation from a solution or order of extent changes in the size and water content of hydrogels[12]. An appropriate proportion of hydrophobicity and hydrophilicity in the molecular structure of the polymer is believed to be required for the phase transition to occur.

Smart polymers could be classified in response to their physical form into three main classes[13, 14],

[A] *Linear free chains in solutions*, where the polymer undergoes a reversible collapse after an external stimulus is applied,

[B] *Chains adsorbed or grafted on a surface*, where the polymer reversibly adsorbs or collapses on a surface, respectively, converting the interface from hydrophilic to hydrophobic, once a specific external parameter is modified and

[C] Covalently *cross-linked gels and reversible or physical gels*, which can be either micro or macroscopic networks and on which swelling behavior is environmentally triggered.

As the stimulus-responsive behavior occurs in aqueous solutions, these polymers and hydrogels are becoming increasingly attractive in biotechnology and medicine, for their uses, as basic components of *biosensors*[15], *"switch on/off" drug release*[16], *drug delivery systems*[19-24], *affinity precipitation*[25-28], *immobilization of* enzymes[29-31], *cells*[32], *tissue engineering*[33] and *artificial muscles*[34].

Poly (N-isopropylacrylamide) (PNIPAM) and its copolymers have been studied extensively as temperature sensitive polymers[35]. Pelton and Chibante[36] reported first time in 1986 synthesis of temperature-sensitive microgel from N-isopropylacrylamide (NIPAM) and N, N'-methylene bisacrylamide (MBA). After that, many research papers were published on copolymeric microgels based on NIPAM with other ionic monomers and these copolymers were used for various biomedical applications[37-55]. Recently, poly(N-vinylcaprolactum) (PVCL), water soluble, biodegradable, temperature responsive polymer having lower critical solution temperature (LCST) near to body temperature (around 32 °C) has attracted much attention of researchers and technologist[56-58]. So far, only a few studies related to its properties and applications have been reported even though PVCL has been commercially available from BASF for a long time. Much of the published work is concentrated on the PVCL based hydrogels as they have potential applications in controlled drug delivery system, separation science, immobilization of enzymes and in oil-recovery technology[59-64]. Similarly, colloidal systems can be equally attractive for such applications, which can be easily synthesized through free radical micro emulsion polymerizations. Tenhu et al have reported synthesis of thermosensetive PVCL microgel by emulsion polymerization using sodium dodecyl sulphate and potassium per sulphate as a surfactant and initiator respectively and extensively studied their molecular properties[65-71].

The present chapter is dedicated to the synthesis and characterization of thermoresponsive poly (MMA-co-VCL) copolymeric nanoparticles and further to explore the possibility of these nanoparticles as a delivery vehicle for model anticancer drug etoposide.

3.2 Experimental

3.2.1 Materials

Etoposide was obtained as a gift sample from CIPLA Limited, Mumbai, India. Etoposide (also commonly known as VP-16) is a semisynthetic derivative of podophyllotoxin used in the treatment of certain neoplastic diseases. It is 4'-dimethylepidophyllotoxin 9-[4,6-0-(R)-ethyllidene-(beta)-D-gludopyranoside]. It is highly soluble in methanol-chloroform mixture, slightly soluble in ethanol, and

sparingly soluble in water and ether. It has molecular weight 588.58 and a molecular formula $C_{29}H_{32}O_{13}$. It has very high protien binding capacity (up to 97 %) and its half life is 4-12 hours.

N-vinylcaprolactam, (VCL) (98%, Sigma-Aldrich, Steinheim, Germany) and methyl methacrylate (MMA) (Merck, Mumbai, India), were distilled under high vacuum and stored at 4 °C prior to use. L-ascorbic acid (AA) (10 % w/v), hydrogen peroxide (HP) (30 % w/v, Merck, Mumbai, India) and sodium dodecyl sulphate (SDS) and polysorbate-80 from SD Fine Chem., Baroda, India were used as received. AR grade methanol, acetone, hexane, tetrahydrofuran and hydroquinone from Merck, India were used as received. Double distilled deionised water (0.22 micron nylon filtered) was used throughout the experiments.

3.2.2 Preparation of poly (MMA-co-VCL) copolymeric nanoparticles

Copolymeric nanoparticles of various compositions were prepared by O/W microemulsion polymerization technique. The ternary microemulsions comprising MMA-VCL monomer mixture (6 % w/w) with monomer weight ratios varying from 90:10 to 40:60 MMA:VCL, SDS (2 % w/w) and water (92 % w/w) were taken in three-neck reaction vessel equipped with a nitrogen inlet, thermometer, water condenser and magnetic stirrer. Typically, monomer mixture to surfactant ratio was kept constant at 3 for all recipes. The ternary micro emulsion was deoxygenated by bubbling purified nitrogen for 15 minutes. Polymerization was initiated by redox initiator pair hydrogen peroxide and L-ascorbic acid at 40 ± 2 °C. MMA was added drop wise to maintain the monomer ratio in feed. The polymerization was continued for 4 hours and resulted into bluish transparent and stable latexes. The polymerization was terminated using sodium nitrate as a free radical inhibitor along with hydroquinone.

- ***Latex Purification***

Latex purification was done as described in section 2.2.2. After removal of unassociated surfactant, the latex was precipitated in 6-8 fold excess volume of diethyl ether. The adsorbed surfactant and homopolymer were removed by washing

the precipitate with water. Copolymer was further purified twice by dissolving the copolymer in small amount of tetrahydrofuran and reprecipitating in n-hexane.

For the determination of reactivity ratio, reactions were carried out as described above and copolymer was collected below 10% conversions. MMA/VCL mole ratios were varied from 90/10, 80/20, 70/30, 60/40, 50/50 and 40/60. The composition of methyl methyacrylate and N-vinylcaprolactam in copolymer was determined from ^{1}H NMR.

3.2.3 Preparation of etopoisde loaded poly (MMA-co-VCL) copolymeric nanoparticles

Etoposide loaded copolymeric nanoparticles of various compositions were prepared by O/W microemulsion polymerization technique. The ternary microemulsions comprising MMA-VCL monomer mixture (6 % w/w) containing 1 % w/w etoposide having monomer weight ratios varying from 100:0, 75:25, 50:50 and 25:75 MMA:VCL, SDS (2 % w/w) and water (91 % w/w) were taken in three-neck reaction vessel equipped with a nitrogen inlet, thermometer, water condenser and magnetic stirrer. Typically, monomer mixture to surfactant ratio was kept constant at 3 for all recipes. The ternary microemulsion was deoxygenated by bubbling purified nitrogen for 15 min. Polymerization was carried out as described in section 3.2.2.

3.2.4 Characterization techniques

3.2.4.a Fourier transform infrared spectrometry (FTIR)

The FTIR spectra of the placebo copolymeric nanoparticles, etoposide loaded copolymeric nanoparticles and etoposide were recorded on a Perkin Elmer Rx_1 IR spectrophotometer using 1-cm-diameter KBr pellets.

3.2.4.b Nuclear magnetic resonance spectrometry (NMR)

^{1}H NMR spectra of homopolymer (PMMA) and copolymer poly (MMA-co-VCL) were recorded using 400 MHz NMR spectrophotometer (Bruker specrospin Avance Ultra-shield, Germany) at room temperature (~30 ± 2 °C). The spectra were obtained after accumulating 32 scans by using 1% sample in $CDCl_3$.

3.2.4.c Gel permeation chromatography (GPC)

Number average ($\overline{Mn}$) and weight average ($\overline{Mw}$) molecular weights of copolymers with different compositions and etoposide loaded copolymers were determined by using Perkin Elmer Totalchrom gel permeation chromatography instrument as described in section 2.2.4.c.

3.2.4.d Cloud point determination

The cloud point of the copolymer solution in double distilled water (0.1 gL^{-1}) was determined by spectrophotometric detection of the changes in turbidity at 500 nm using Perkin Elmer lambda 35 UV-VIS spectrophotometer. The water-jacketed sample and reference cell holders were coupled with a Julabo 5A circulating bath having a digital temperature controller attached to it. Heating rates were 0.5 °C / min and double distilled deionised water was used as reference. Cloud point was considered as the temperature corresponding to a 10% reduction in the original transmittance of the solution[72].

3.2.4.e Differential scanning calorimetry (DSC)

Differential scanning calorimetric (DSC) analysis was carried out using a Mettler–Toledo 822 instrument (Greifensee, Switzerland). The instrument was calibrated using indium as a standard and samples were heated in sealed aluminum pans between 30 to 400°C at a heating rate of 10°C min^{-1}.

3.2.4.f Powder X-ray diffraction (XRD)

Powder X-ray diffraction (XRD) of the placebo copolymeric nanoparticles, etoposide loaded copolymeric nanoparticles, etoposide and physical mixture of etoposide and placebo copolymeric nanoparticles were recorded on a Philips X'pert multipurpose diffreactometer (MPD range, Germany) using a Ni-filtered Cu Kα radiation (1.5405 A°) over the 2θ range of 3-100°. The Philips X'pert MPD is a powder diffractometer, which is used primarily for phase analysis and determination of crystal structure.

3.2.4.g Dynamic light scattering (DLS)

Particle size of the synthesized copolymeric nanolatex was determined using dynamic light scattering technique as described in section 2.2.4.d. The sample was diluted 10 times with double distilled deionised water before measurements.

3.2.4.h Transmission electron microscopy (TEM)

TEM analysis of copolymeric nanoparticles and drug loaded nanoparticles was performed using JEOL 1200 EX Transmission Electron Microscope at accelerating voltage of 80 kV. One drop of latex was dispersed in 5 mL of water and was placed on the carbon coated copper grid. The grid was dried under IR lamp and then the images of representative areas were captured at suitable magnifications.

3.2.4.i Estimation of percentage encapsulation efficiency

The UV spectra of the purified copolymers, drug and etoposide loaded copolymers were recorded on a Perkin Elmer Lambda 35 UV/Vis spectrophotometer. The drug loaded nanoparticles were purified by successive washings with methanol to remove the adsorbed drug and then re-lyophilized for a period of 24 h in order to get dry nanoparticles. Ten milligrams of nanoparticles were dissolved in ten mL of chloroform. Entrapment efficiency of etoposide in nanoparticles was calculated from the calibration plot constructed at 293 nm after confirming the noninterference of polymers in the absorption region of etoposide.

3.2.4.j In-vitro release

In-vitro release study for etoposide loaded polymeric nanoparticles of various compositions was carried out in a dialysis bag (cut-off 10,000, Hi-Media, India) diffusion technique[73]. Etoposide release from the nanoparticles was studied in phosphate buffer of pH 7.4 containing 0.1 % Tween 80. The aqueous nanoparticulate dispersion equivalent to 1 mg etoposide was placed in cellulose dialysis bag and was sealed at both ends. The dialysis bag was immersed in the receptor compartment containing 50 mL of the dissolution medium, and stirred at 100 rpm under magnetic stirring. Aliquots of samples were withdrawn at regular time intervals and equivalent volume was replaced with fresh dissolution medium. The samples were analyzed by

measuring absorbance at 293 nm against reagent blank. All experiments were repeated thrice and the average values were considered.

3.2.4.k In-vitro cytotoxicity

Cell culture

B16F10, a highly metastatic lung selected subline derived from C57/BL6 murine melanoma, was purchased from National Centre for Cell Science (NCCS, Pune, India). The cell line was maintained as a continuous culture in Iscove's minimum Dulbecco's medium (IMDM; GIBCO, BRL, MD, USA) supplemented with 10 % fetal bovine serum (GIBCO BRL), 100 units/mL penicillin and 100 µg/mL streptomycin. Cells were grown in a humidified atmosphere of 5 % CO_2 and 95 % air at 37 °C. Media was replenished every third day.

Cytotoxicity assay

Cytotoxicity of the placebo copolymeric nanoparticles and etoposide loaded copolymeric nanoparticles was evaluated using B16F10 melanoma cell lines. Cells were seeded in 96-well microplates at a density of 5 X 10^3 cells/well. Cells were allowed to grow and stabilize for 24 h. They were then treated with series of dilutions of different composition's poly (MMA-co-VCL) copolymer nanoparticles for 24 hrs in order to find their cytotoxic effect. The prepared nanoparticles being assayed were added directly to the medium in each well at the 0.00001-0.5 mg/mL. On each 96-well plates, four wells were left untreated for use in calculating the 100 % OD values. Post treatment cell viability was determined by colorimetric assay using 3-(4, 5-dimethyl-2-thiazolyl)-2, 5-diphenyltetrazolium bromide (MTT). MTT reagent (Sigma Aldrich) was added to each well to make a final concentration of 1 mg/mL of media and incubated for 4 h at 37 °C. Formazan crystals were dissolved in 100 µL of DMSO; the optical density was measured in the enzyme-linked immunosorbent assay plate reader (Molecular Devices, Spectra Max 190 with Soft max Pro) at 540 nm with a reference wavelength of 690 nm. Similarly, cytotoxicity assay of serial dilution of different compositions of plain etoposide and etoposide loaded copolymeric nanopartiucles was done.

3.3 Results and Discussion

3.3.1 Representative FTIR spectra of poly (MMA-co-VCL) copolymers

FTIR spectra of placebo copolymeric nanoparticles, free etoposide and etoposide loaded copolymeric nanoparticles were recorded and are given in ***Figure 3.1.***

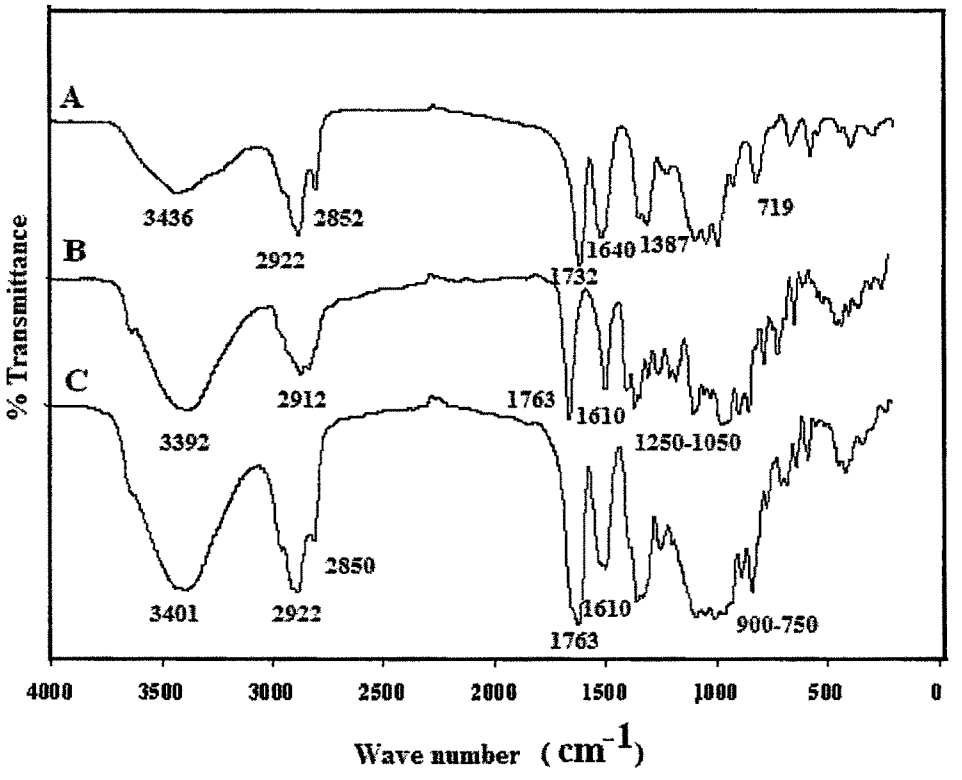

Figure 3.1 FTIR Spectra of (A) Poly (MMA-VCL) copolymer, (B) etoposide and (C) etoposide loaded copolymeric nanoparticles.

The carbonyl stretching vibrations of the MMA and VCL units of the copolymer ***(Figure 3.1A)*** appear as a very strong absorption bands at 1732 cm^{-1} and 1640 cm^{-1}, respectively. The strong and broad band appearing at 3436 cm^{-1} may be due to water of hydration attached to the polymer as product being hydrogel in nature[56]. The bands at 2922, 2852, 1447 and 1387 cm^{-1} are attributed to stretching and bending vibrations of $-CH_2$, -CH groups respectively. Bands appearing at 1045 cm^{-1},

1245 cm^{-1} correspond to C-O-C ester stretching vibration of acrylate polymer and bands appearing at 719 cm^{-1} correspond to the presence of more than three -CH_2 groups in a cyclic structure, providing evidence of copolymerization. The infrared spectra of etoposide ***(Figure 3.1B)***, exhibits strong absorption peaks at 3392, 2912, 1763 -1610, 1500-1300, 1250-1050 and 950-850 cm^{-1} corresponding to –OH, -CH_2 stretching, lactone group, ring stretching, C-O-C linkages and AR-CH functional groups respectively as reported earlier[73]. While in the case of etoposide loaded copolymeric nanoparticles ***(Figure 3.1C)***, presence of characteristics bands of drug and copolymer at 3401, 2922, 2852, 1763-1610, 1520-1300, 1250-1050 and 900-750 cm^{-1} correspond to –OH, -CH_2 stretching, lactone group, ring stretching, C-O-C linkages and more than three -CH_2 groups in cyclic structure confirm the entrapment of etoposide in nanoparticles.

3.3.2 Determination of reactivity ratio

Reactivity ratios for MMA-VCL monomer pair were determined by linear least square and nonlinear least square methods. Details of the methods used are given in section 2.3.2. The high resolution ^1H NMR spectrum of homopolymer (PMMA) and copolymer, poly (MMA-co-VCL) are shown in ***Figure 3.2.*** The composition of the copolymer was determined by the well separated signals that appeared at 4.798 ppm corresponding to the proton from a caprolactam ring of the VCL units and the signal that appeared near 0.842 ppm corresponding to the methyl proton of the MMA units. This also provides evidence for copolymerization. Similar results are reported earlier by Qiu and Sukhishvili[58] for the copolymerization of vinyl caprolactam with glycidyl methacrylate (GMA) through solution polymerization technique. The composition of the copolymer was evaluated from the relative intensities of methyl group of MMA and caprolactam ring of the VCL units and the results obtained are summarized in ***Table 3.1.***

Table 3.1 Mole fractions of monomers in feed and copolymers.

(MMA:VCL) mole ratio in feed	Mole fractions in feed		Mole fraction in copolymer calculated from ^{1}H NMR		% Conversion
	M_{MMA}	M_{VCL}	P_{MMA}	P_{VCL}	
90:10	0.9	0.1	0.96	0.04	4.7
80:20	0.8	0.2	0.92	0.08	3.9
70:30	0.7	0.3	0.9	0.1	6.7
60:40	0.6	0.4	0.8	0.2	6.2
50:50	0.5	0.5	0.7	0.3	7.9
40:60	0.4	0.6	0.69	0.31	5.5

M_{MMA} =Mole fraction of MMA in feed, M_{VCL} = Mole fraction of VCL in feed
P_{MMA} = Mole fraction of MMA in copolymer, P_{VCL} =Mole fraction of VCL in copolymer.

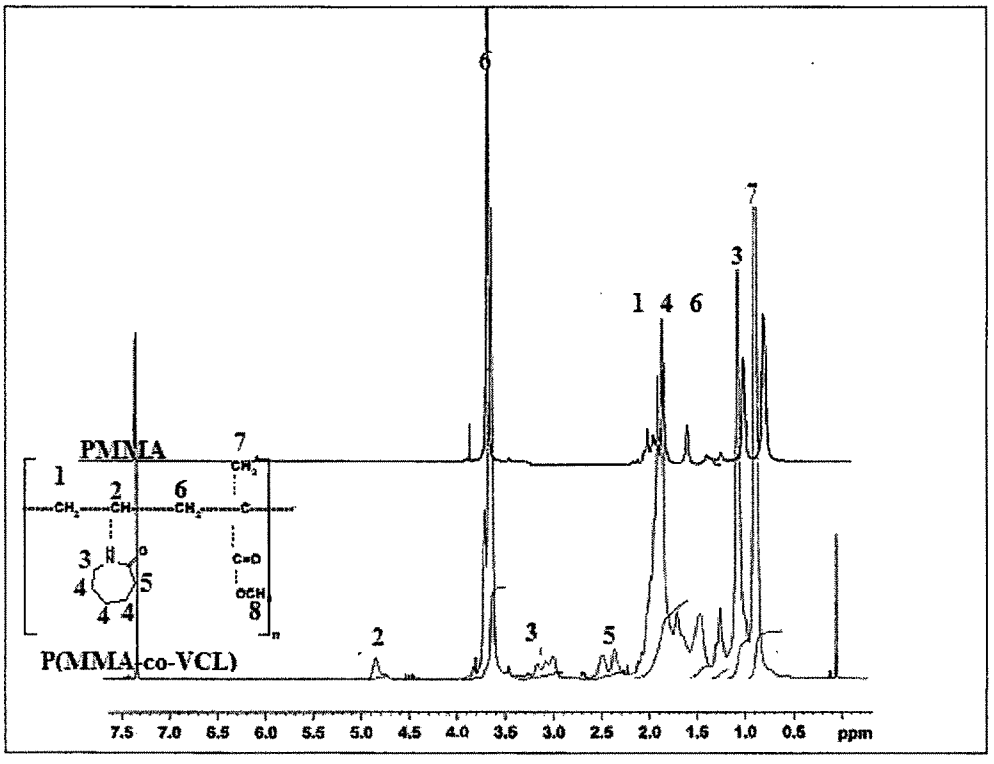

Figure 3.2 ^{1}H NMR spectra of PMMA and poly (MMA-VCL) copolymer.

- **Fineman-Ross method**

Fineman-Ross (FR) and Inverted Finneman-Ross (IFR) linear least square methods[75] were used to determine the reactivity ratios of MMA-VCL monomer pair. ***Figure 3.3 and 3.4*** are the linear plots obtained by using the FR methods equation as described in section 2.3.2. The calculated parameters necessary in determination are given in ***Table 3.2***. The obtained values of r_{MMA} and r_{VCL} by these methods were 2.63, 2.68 and 0.19 and 0.39 respectively.

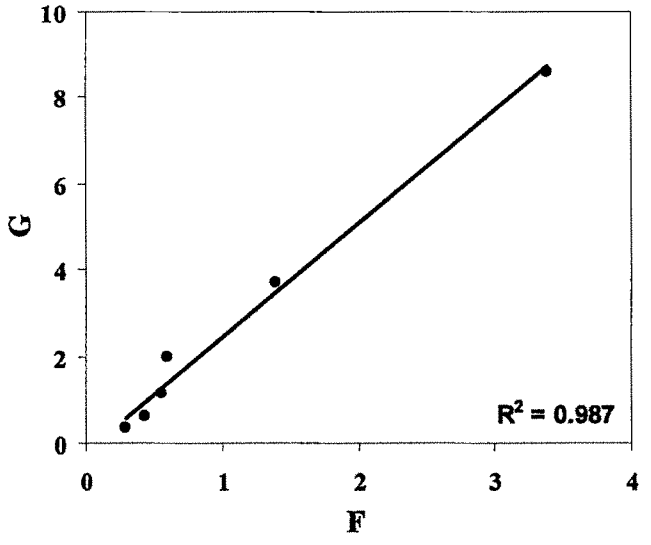

Figure 3.3 Fineman-Ross methods.

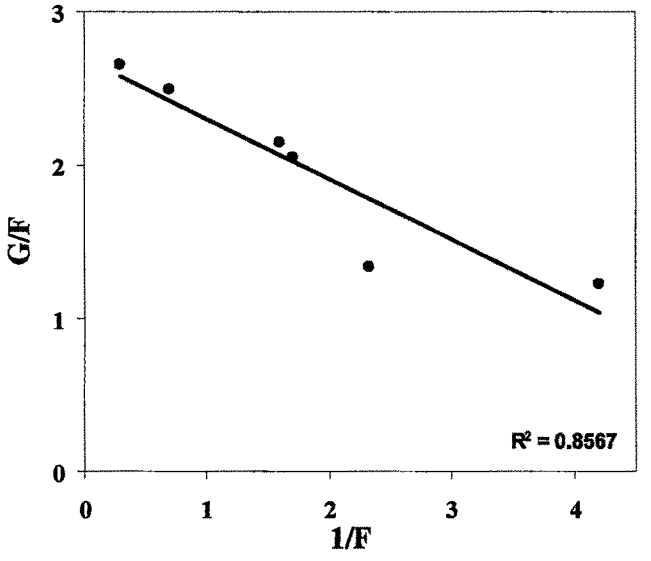

Figure 3.4 Inverted Fineman-Ross method.

- **Mortimer-Tidwell method**

A modification or extension of curve fitting method proposed by Tidwell and Mortimer[76], which they called the non-linear least-square method and is considered to be one of the most accurate procedures for determination of monomer reactivity ratios, was used for the determination of reactivity ratio determination of MMA-VCL monomer pair. Details of the method are given in section 2.3.2.

A brief description of the method consists, initial estimates of r_{MMA} and r_{VCL} a set of computations performed yielding the sum of the squares of the differences between the observed and computed polymer compositions. The summation is then minimized by iteration, yielding reactivity ratio. By this method, the reactivity ratio values obtained for r_{MMA} and r_{VCL} are 2.63 and 0.25 and are graphically represented in ***Figure 3.5***. It was well reported in the literature that the product of r_{MMA} and r_{VCL} decides the character of the obtained copolymer. Here in this case the product of r_{MMA} and r_{VCL} was observed to be less than 1 indicating the tendency of copolymer to be random in nature.

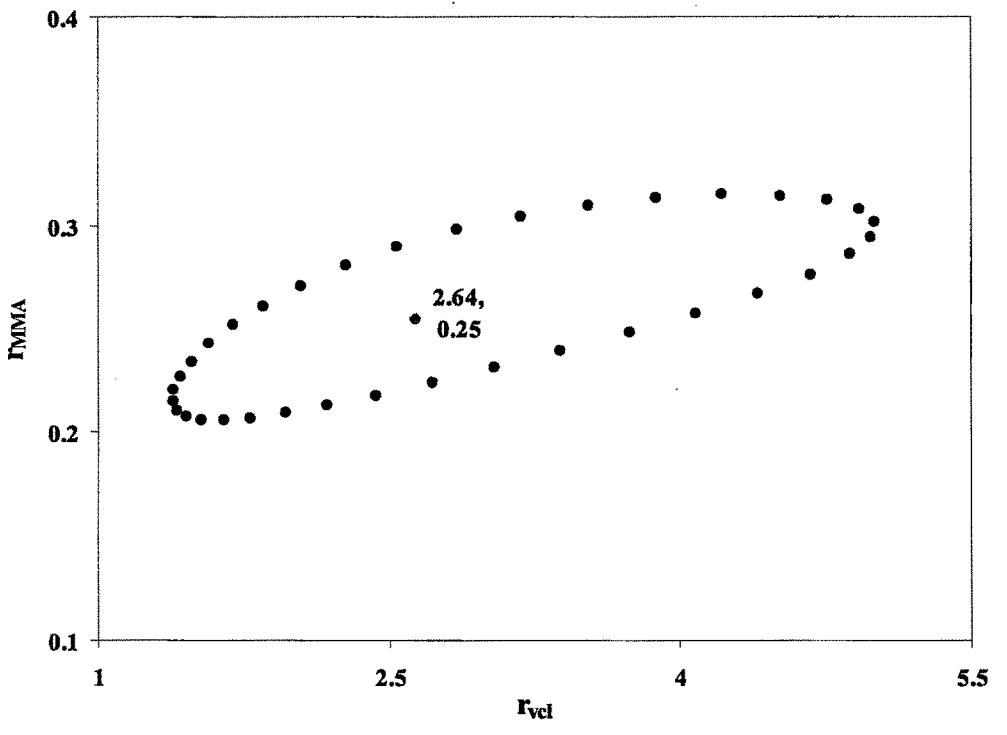

Figure 3.5 Tidwell-Mortimer nonlinear least square method.

Table 3.2 The calculated parameters needed for the determination of reactivity ratios at < 8 % conversion.

(MMA:VCL) mole ratio in feed	M	P	G	F	G/F	1/F
90:10	9	24	8.62	3.37	2.55	0.29
80:20	4	11.5	3.65	1.39	2.62	0.72
70:30	2.33	9	2.07	0.60	3.43	1.65
60:40	1.5	4	1.12	0.56	2	1.78
50:50	1	2.3	0.57	0.43	1.3	2.33
40:60	0.66	2.2	0.36	0.29	1.2	4.19

M_{MMA} = Mole Fraction of MMA in Feed

M_{VCL} = Mole Fraction of VCL in Feed

P_{MMA} = Mole Fraction of MMA in Copolymer

P_{VCL} = Mole Fraction of VCL in Copolymer

M = M_{MMA} / M_{VCL}

P = P_{MMA} / P_{VCL} (calculated from Table 3.1)

G = $M (P-1) / P$

F = M^2 / P

3.3.3 Molecular weight determination

Table 3.3 summarizes the molecular weight and polydispersity of the synthesized copolymers. The molecular weights of the synthesized copolymers as estimated by using Polystyrene standard were in the range of 5-20 X 10^4 and polydispersity was in the range of 1.3-1.6. It was observed that as the VCL content increases in the copolymer, the peak molecular weight of the copolymer decreases and polydispersity increases as observed in ***Figure 3.6*** and ***Table 3.3.***

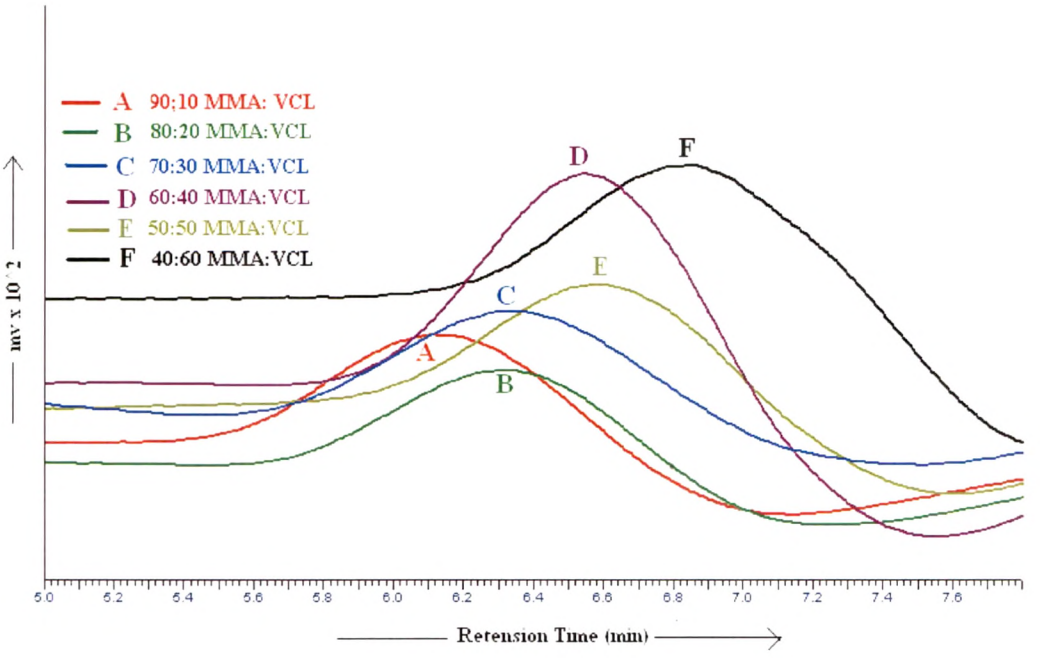

Figure 3.6 Effect of copolymer composition on molecular weight distribution by GPC.

Table 3.3 Molecular weight, particle size and phase transition temperature of the copolymer latexes.

Copolymer (MMA:VCL)	Particle Size (nm)	$\overline{Mw}$ X 10^{-4}	$\overline{Mn}$ X 10^{-4}	PDI	Phase transition temperature (°C) By UV-VIS spectrometry
PMMA	18	78.3	66.5	1.17	--
90:10	20	20.1	14.2	1.42	62
80:20	23	14.1	10.5	1.33	52
70:30	32	13.5	9.5	1.43	52
60:40	34	9.1	6.7	1.35	44
50:50	39	10.3	6.48	1.59	38
40:60	42	5.46	3.56	1.53	36

Similar observation was reported earlier by Qui and Sukhishvili[58] for the copolymerization of vinyl caprolactam with glycidyl methacrylate (GMA) through solution polymerization technique. The molecular weights of the synthesized copolymers, as estimated with PEO standards, were in the range of 50–100 K with a polydispersity of 1.6. They also reported that, the two copolymers displayed a bimodal molecular weight distribution, which was attributed to drop wise addition of GMA in the reaction process. While in our case dropwise addition of MMA in reaction mixture didn't show any bimodal distribution in entire synthesized composition range through a continuous gradual feeding micro emulsion polymerization technique, and resulted in more homogeneous composition.

Gel Permeation Chromatographic analysis of the etoposide loaded nanoparticles is given in ***Figure 3.7.*** It was observed in the graph that, molecular weight decreases and polydispersity index increases with increase in VCL content in

copolymer. The molecular weight and polydispersity data are given in ***Table 3.5***. Peak molecular weight and polydispersity were found to be 1.6 – 0.48 x10^5 and 1.05 -1.33 respectively. Here, we can observe that, presence of etoposide during polymerization reduces molecular weight of the synthesized polymers.

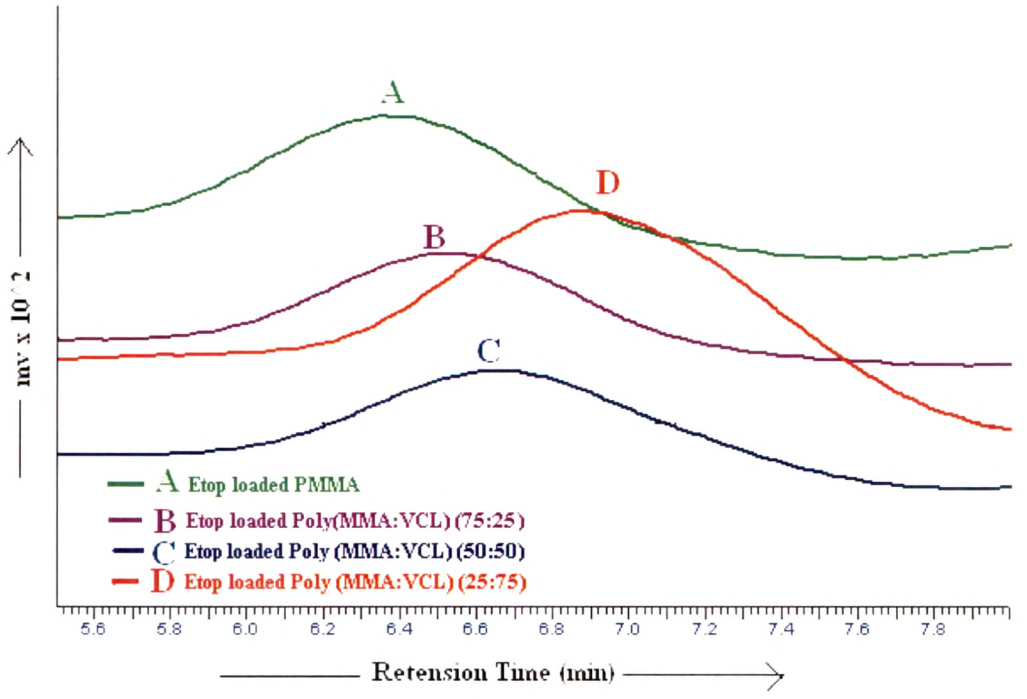

Figure 3.7 Effect of etoposide on molecular weight distribution of copolymer by GPC.

3.3.4 Cloud point determination

The temperature dependant phase separation of aqueous solutions of different compositions of poly (MMA-co-VCL) copolymer was investigated by visible spectrophotometry at 500 nm. ***Figure 3.8*** shows percentage transmittance vs temperature curves for three poly (MMA-co-VCL) compositions.

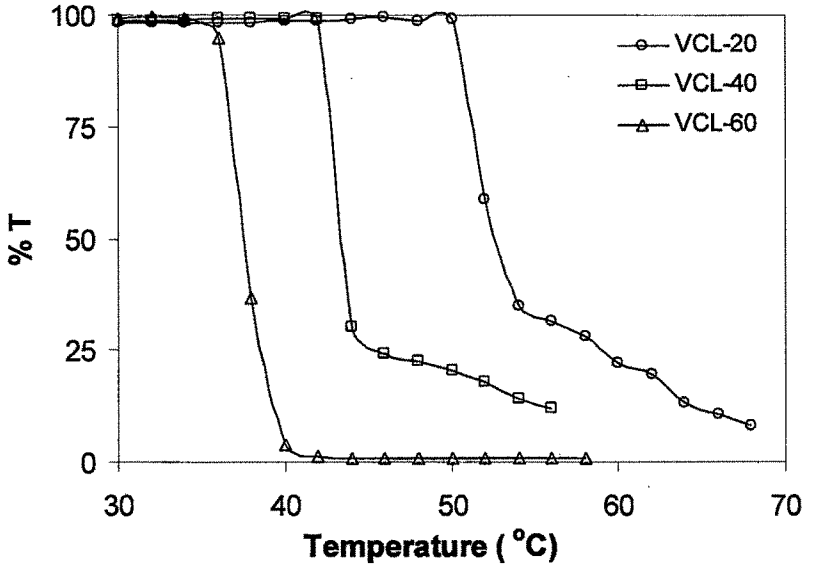

Figure 3.8 Percentage transmittance at 500 nm of aqueous solution containing 0.1 mg/mL poly (MMA-co-VCL) solution at different temperatures. (O) 80:20 (MMA: VCL), (□) 60:40 (MMA: VCL), (Δ) 40:60 (MMA: VCL).

Usually, a sample is transparent when its transmittance, (I/I_0), is greater than 95% and becomes totally opaque when its transmittance, (I/I_0), is less than 75 %. In the present work, the temperature corresponding to a 10 % reduction in transmittance was used as a measure of the cloud point[77]. The copolymer compositions and their corresponding phase separation temperature are given in ***Table 3.3***. It was reported earlier that, a cloud point of PVCL strongly depends on the molecular weight and composition of the polymer in the case of copolymer. Yin and Stover[77] have reported strong dependence of phase transition temperature on copolymer composition. While the dependence of phase transition temperature of the thermo sensitive polymers on

their molecular weight is a matter of dispute. Fujishige *et al*[78] and Lessard *et al*[79] found that the phase separation temperature of polyNIPAAM is independent of the molecular weight or the concentration. They argued that the coil-to-globule transition takes place solely depending on the temperature of aqueous polymer solution at the initial stage of the phase separation, followed by the onset of aggregation of individual chain molecules mainly due to the intermolecular interaction between the hydrophobic groups distributed on the surface of the resulting globular particles of the polymer in aqueous solution. According to Schild *et al* [80, 81], who studied the phase transition of polyNIPAAM samples, an increase in the phase separation temperature is to be expected with decreasing molecular weight and they argued that at higher concentration, the coil-to-globule transition is followed by globular aggregation through intermolecular interactions. They have argued that, molecular weight should have an influence on cloud temperature, as the overlapping concentration is dependent on the chain length. The decrease in the phase separation temperature with increasing molecular weight has not been established only for polyNIPAAM but also for other thermo sensitive polymers such as polyDEAAM [81, 82]. Apart from the molecular weight influence, the differences between phase transition temperature may also arise from the polymer samples used (i.e. polymer samples concentration) and/or the conditions i.e. heating rate, experimental technique used in the measurements. Idziak *et al*[83] have observed that an increase in heating rate results in a shift in phase separation temperature towards higher side. While Boutris *et al* [72] pointed out that at low concentrations the polymer particles fail or are slow to aggregate to a size that can be detected by the spectrophotometer.

In the present case, it was observed that, aqueous solutions of copolymers with more than 40 mol % VCL show thermal phase transition near to body temperature (< 44 °C) at heating rate 0.5 °C/min and polymer concentrations 0.1 g/L. Hence heating rate and polymer sample concentration are important factors in the cloud point determination. As reported earlier difficulty in determination of cloud point temperature at low concentration of PNIPAM based samples, in the present case, such difficulties were not observed for the synthesized copolymeric nanoparticles.

3.3.5 Differential scanning calorimetry

DSC thermograms of (A) etoposide, (B) lyophilized copolymeric nanoparticles, (C) physical mixture of etoposide and copolymeric nanoparticles and (D) etoposide loaded copolymeric nanoparticles are given in ***Figure 3.9.***

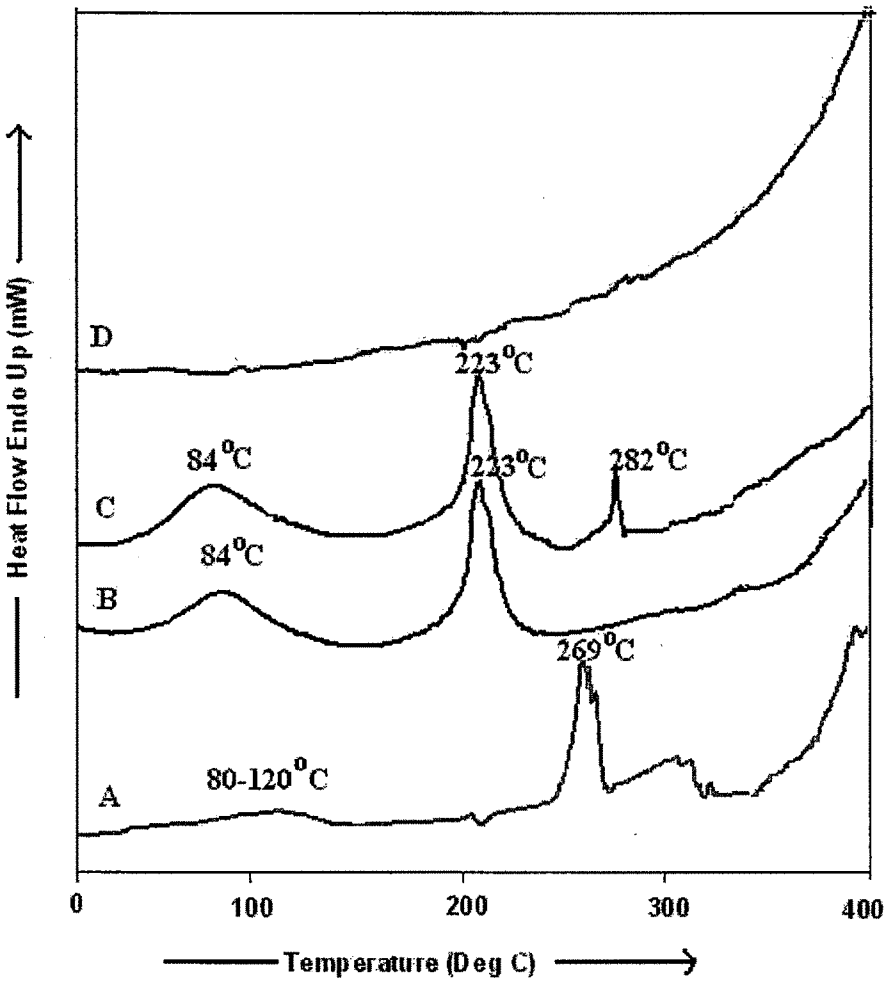

Figure 3.9 DSC thermograms of (A) etoposide, (B) lyophilized copolymeric nanoparticles, (C) physical mixture of etoposide and copolymeric nanoparticles and (D) etoposide loaded copolymeric nanoparticles.

DSC thrmogram of pure etoposide (A) evidenced an endotherm over the range of 80-120 °C due to dehydration of water molecules followed by a recrystallisation at 208 °C and melting at 269 °C followed by decomposition above 290 °C. A similar

observation is reported by Jasti *et al* [84]. While endothermic peaks at 84 °C and 223 °C are clearly observed for lyophilized copolymeric nanoparticles (B). However, endothermic peaks at 84 °C and 269 °C corresponding to copolymer and etoposide were not observed in DSC plot of the etoposide loaded nanoparticles (D), but separate endothermic peaks at 84 °C and 284 °C corresponds to copolymeric nanoparticles and etoposide were observed in a physical mixture of copolymeric nanoparticles and etoposide (C) confirming that the etoposide is molecularly dispersed in the polymeric matrix (D). Similar observation was reported earlier by Babu *et al*[85]. From these results we can also say no distinct interaction takes place between drug and polymers.

3.3.6 Powder X-ray diffraction (XRD)

Powder X-ray diffraction (XRD) patterns for the (A) etoposide, (B) copolymeric nanoparticles and (C) etoposide loaded copolymeric nanoparticles are given in ***Figure 3.10.***

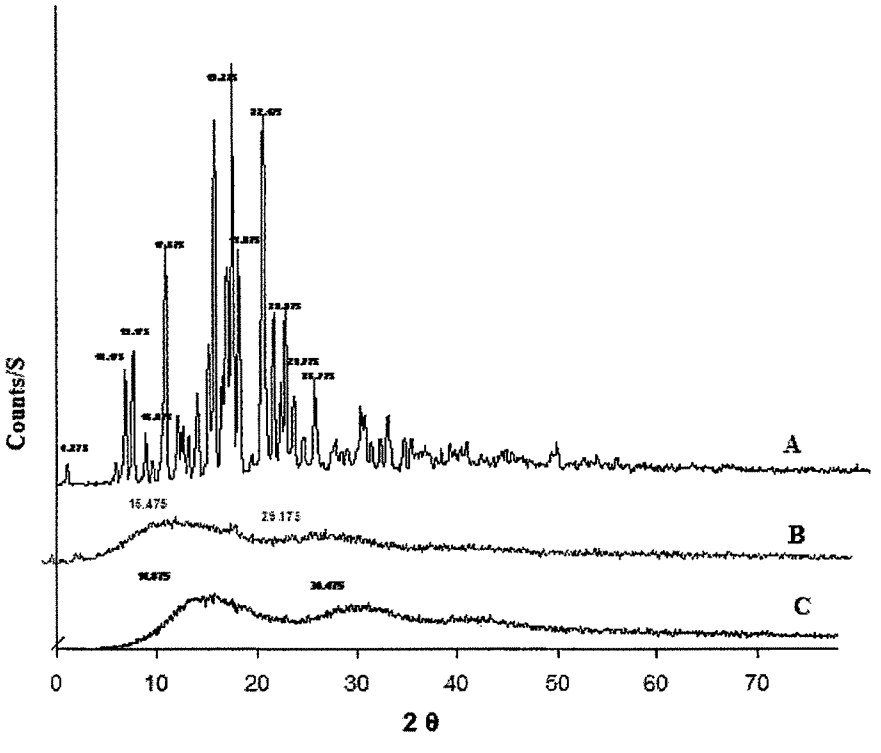

Figure 3.10 X-ray diffraction patterns of (A) etoposide, (B) copolymeric nanoparticles and (C) etoposide loaded copolymeric nanoparticles.

The peaks of interest for pure drug observed at 4.2, 9.46, 10.22, 13.18, 16.15, 17.08, 17.67, 19.26, 19.89, 22.14, 23.03, 23.67, 24.17, 26.78, indicate highly crystalline nature of the drug. While for etoposide loaded copolymeric nanoparticles, all the crystalline peaks of drug diminish, indicating molecular level dispersion of drug in the polymer matrix. These results are in agreements with the earlier published work[86].

3.3.7 Particle size analysis

Particle size and morphology of the poly (MMA-co-VCL) copolymeric nanolatex was determined through Brookhaven's 90 plus dynamic light scattering equipment. A representative particle size histogram obtained through DLS for 90:10 and 50:50 poly (MMA-co-VCL) copolymeric nanolatex are given in ***Figure 3.11*** (A) and (B). The particle size was observed to be between 20-45 nm for all copolymer compositions and the data is compiled in ***Table 3.3***. Particle size was observed to increase with VCL content. All the nanolatexes were kept at room temperature for a period of six months and periodically its particle size was measured in order to see the stability of the latex synthesized. ***Table 3.4*** shows the stability of copolymeric nanolatex with respect to time at room temperature. Particle size showed some increase with increasing incorporation of VCL unit in copolymer. Up to one month storage, no agglomeration of nanoparticles was observed. However with increasing storage time, percentage increment in particles size after six months was observed to be 20-30 % in majority of compositions except 90:10 (MMA: VCL) composition.

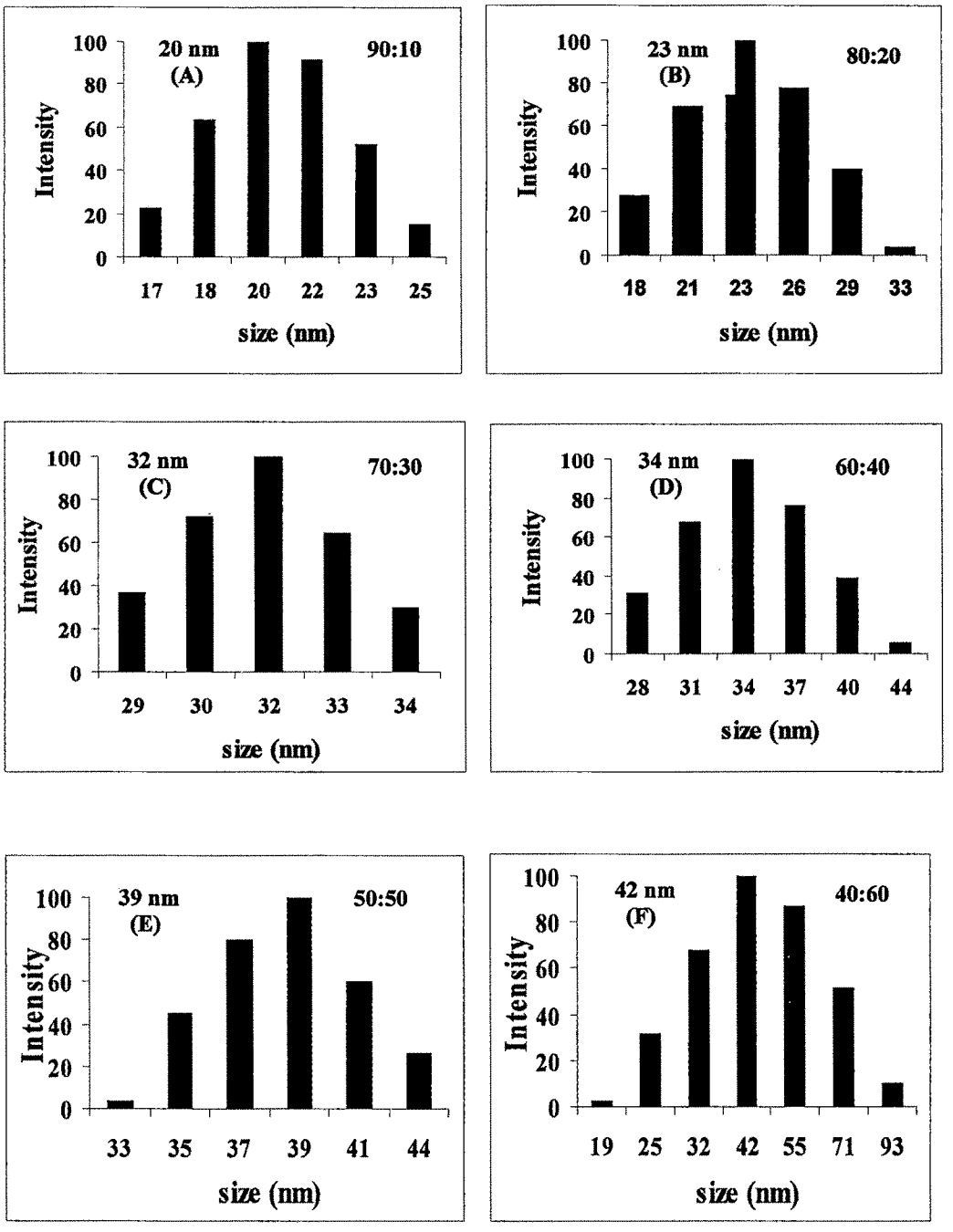

Figure 3.11 **Representative DLS histogram of poly (MMA-co-VCL) copolymer systems (A) (90:10) MMA-co-VCL, (B) (80:20) MMA-co-VCL, (C) (70:30) MMA-co-VCL, (D) (60:40) MMA-co-VCL, (E) (50:50) MMA-co-VCL, (F) (40:60) MMA-co-VCL.**

Table 3.4 Time dependency of the hydrodynamic radius with respect to VCL content at 30 ± 2 ^{0}C.

Copolymer Composition (MMA:VCL)	Particle Size (nm)					
	0 month	One month	Two months	Three months	Six months	% Increment after 6 months
90:10	20	22	21	24	28	40
80:20	23	20	21	24	28	20
70:30	21	22	25	27	28	38
60:40	31	31	33	35	37	20
50:50	32	32	33	38	39	20
40:60	42	42	45	43	54	30

Particle size of the etoposide loaded copolymeric nanoparticles was determined through dynamic light scattering technique. The particle size histograms obtained through DLS for homopolymer (PMMA), and 75:25, 50:50, 25:75 poly (MMA-co-VCL) copolymers are shown in ***Figure 3.12*** and data for drug loaded copolymeric nanoparticles for all compositions are compiled in ***Table 3.5.*** Particles were observed to be in the range of 20-120 nm diameters for etoposide loaded nanoparticles.

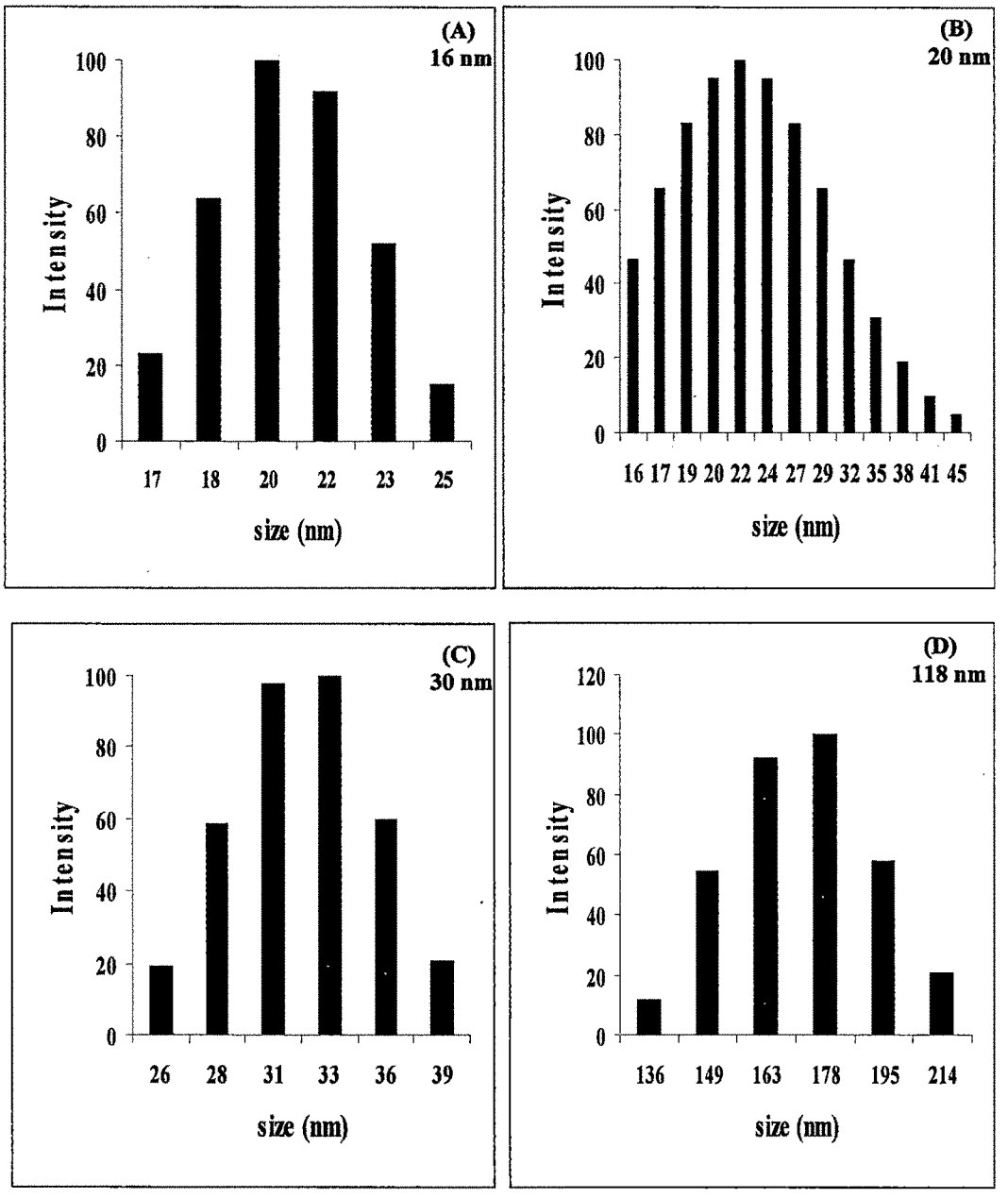

Figure 3.12 **Representative DLS histogram of etoposide loaded copolymeric nanoparticles (A) PMMA, (B) 75:25 poly (MMA-co-VCL), (C) 50:50 poly (MMA-co-VCL) and (D) 25:75 poly (MMA-co-VCL).**

Table 3.5 Particle size, molecular weight distribution and encapsulation efficiency of etoposide in etoposide loaded copolymeric nanoparticles

Copolymer (MMA:VCL)	Particle Size (nm)	$\overline{Mw}$ X 10^{-4}	$\overline{Mn}$ X 10^{-4}	PDI	Encapsulation Efficiency (%)
PMMA	16.3	1.58	1.52	1.05	67
75:25	20.0	0.83	0.74	1.16	45
50:50	30.0	0.75	0.60	1.24	40
25:75	118.0	0.48	0.36	1.33	35

3.3.8 Transmission electron microscopy

Transmission electron microscopy was used to examine size and morphology of copolymeric nanoparticles. ***Figure 3.13 (A)*** shows TEM photographs of 50:50 poly (MMA-co-VCL) copolymeric nanoparticles. The particle size observed from TEM analysis was approximately in the range of 30 ± 5 nm and it was supported by the results obtained from dynamic light scattering technique. Image for 50:50 poly (MMA-co-VCL) copolymeric nanoparticles shows uniformly dispersed nearly spherical nanoparticles.

While in the case of etoposide loaded 50:50 poly (MMA-co-VCL) copolymeric nanoparticle ***(Figure 3.13B)***, particle size was observed to be in the range of 25 ± 5 nm with spherical morphology and monodispersed nature. These results are well supported by the results obtained from DLS analysis.

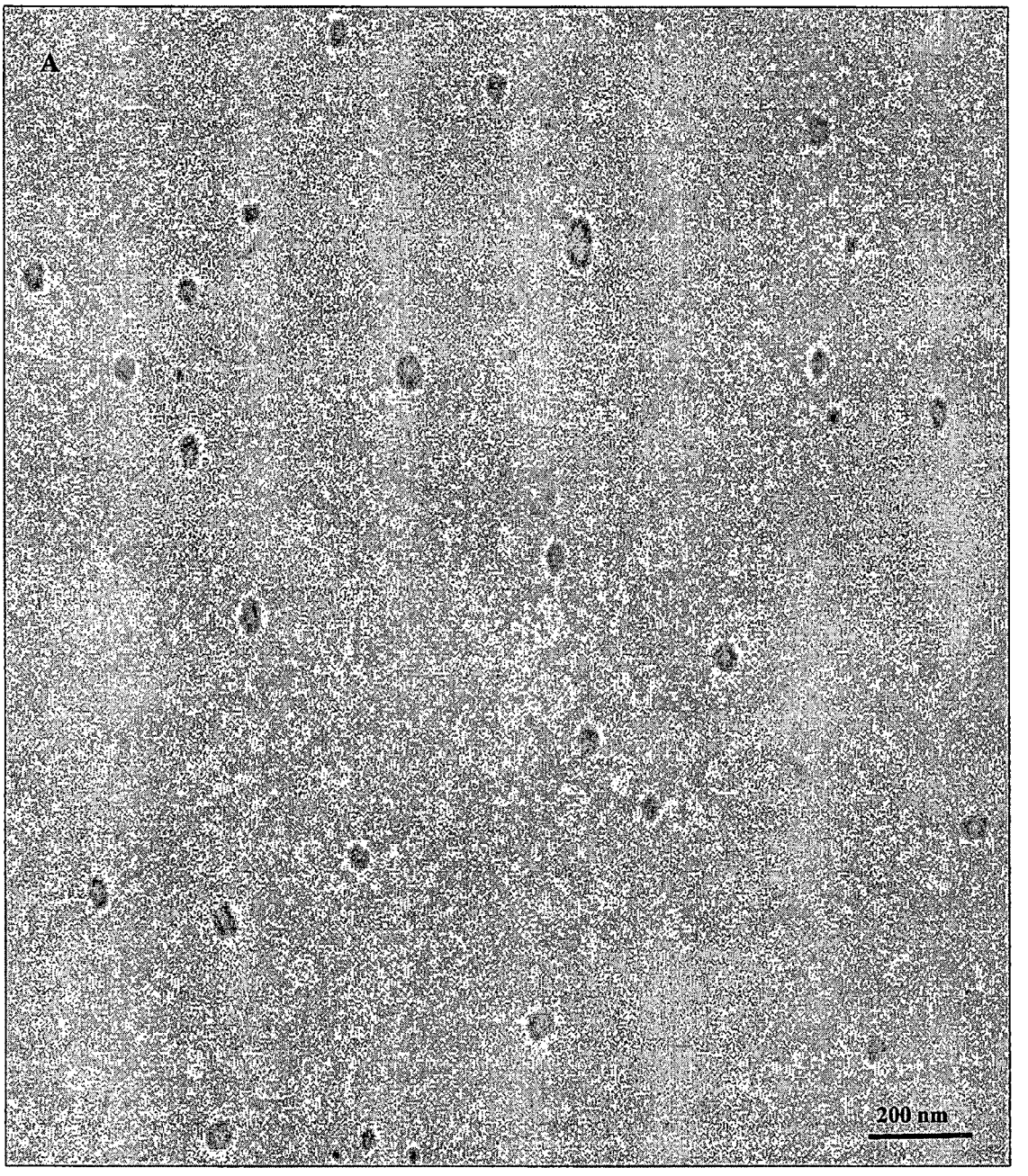
A
200 nm

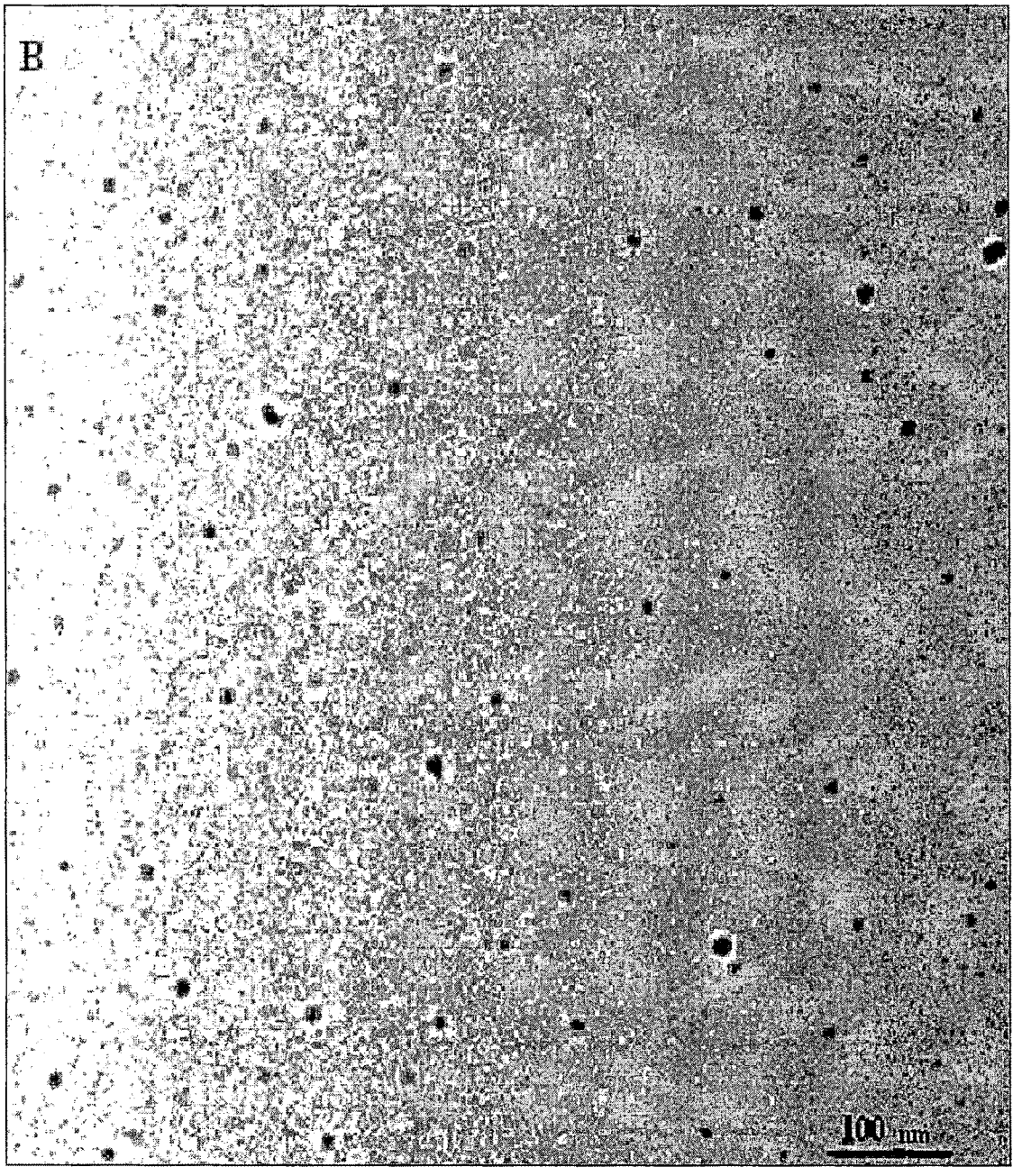

Figure 3.13 TEM images of (A) 50:50 poly (MMA-co-VCL) and (B) etoposide loaded 50:50 poly (MMA-co- VCL) copolymer system.

3.4.9 Entrapment efficiency of etoposide in nanoparticles

The entrapment efficiency of etoposide in copolymeric nanoparticles was determined by using UV spectrometry ***(Figure 3.14).*** The entrapment efficiency was found to be varying from 35-68 % when 1% etoposide was added during polymerization of different monomer compositions. UV-spectrum of pure etoposide ***(Figure 3.14A)*** shows maximum absorbance (λ_{max}) around 293 nm in chloroform, while UV-spectrum of placebo nanoparticles did not show any peak in the UV-Visible region ***(Figure 3.14B)***. UV spectrum of etoposide loaded copolymeric nanoparticles ***(Figure 3.14C)*** shows that, peaks corresponding to drug show small red shift and exhibit maximum absorption at 296 nm. From the calibration plot at 293 nm, entrapment efficiency of etoposide in nanoparticles was calculated. Maximum entrapment (68 %) of etoposide was observed in PMMA. ***Table 3.5*** shows the results of entrapment efficiency of etoposide in nanoparticles of different compositions. It was observed that with increase in the VCL content in copolymerization recipe, encapsulation efficiency of etoposide decreases. This may be due to highly hydrophobic nature of etoposide hesitates to go in the nanoparticle matrix. The entrapment efficiency of etoposide was also observed to be higher for smaller size particles.

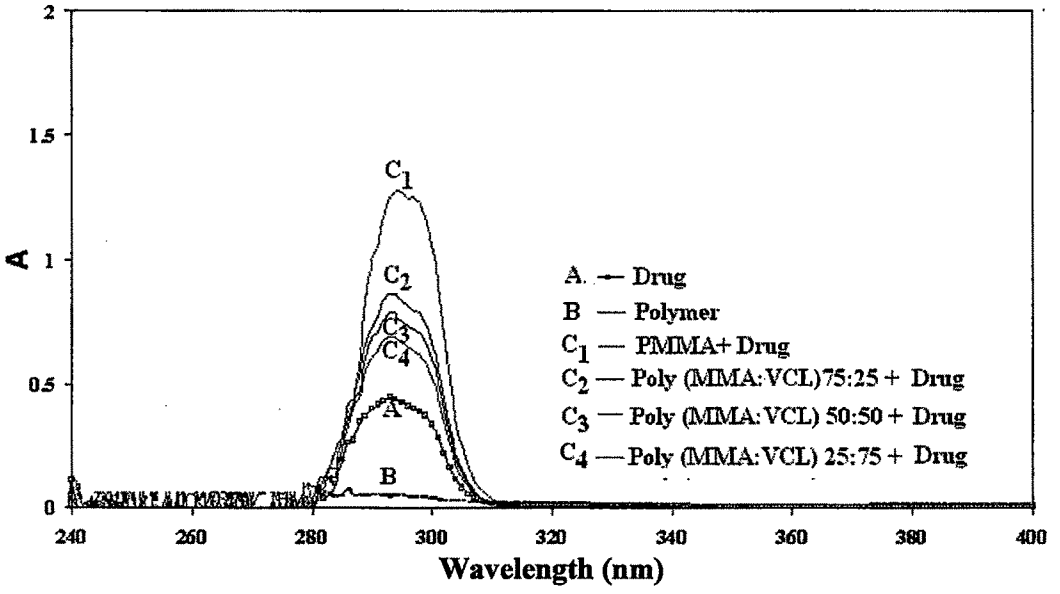

Figure 3.14 UV spectra of (A) etoposide, (B) copolymeric nanoparticles and (C_{1-4}) etoposide loaded copolymeric nanoparticles.

3.4.10 In-vitro release

The release of etoposide from copolymeric nanoparticles in phosphate buffer of pH 7.4 containing 0.1 % Tween 80 is illustrated in ***Figure 3.15.*** The release profile of etoposide from nanoparticles was observed to be biphasic. The first phase shows initial high rate of release for maximum period of 60 min followed by the slow release phase. The total percentage cumulative release was up to the maximum of 82 % for the batches with 25:75 poly (MMA: VCL) and the minimum of 63 % for PMMA for a period of 30 h indicating a sign of controlled release of etoposide. The initial fast release of drug is the outcome of burst release due to the fast dissolution and quick diffusion of drug particles migrated to the periphery during the formation of the particles. A drug like etoposide has low partition co-efficient (1.7) at acidic pH and diffuses faster in the hydrophilic polymer matrix than in a hydrophobic polymer matrix. A similar observation is seen in the present case where polymers with higher hydrophobic character (100 % PMMA) show lower burst release of etoposide (~ 5 %) with respect to low hydrophobic (25 % PMMA) nature copolymeric nanoparticles.

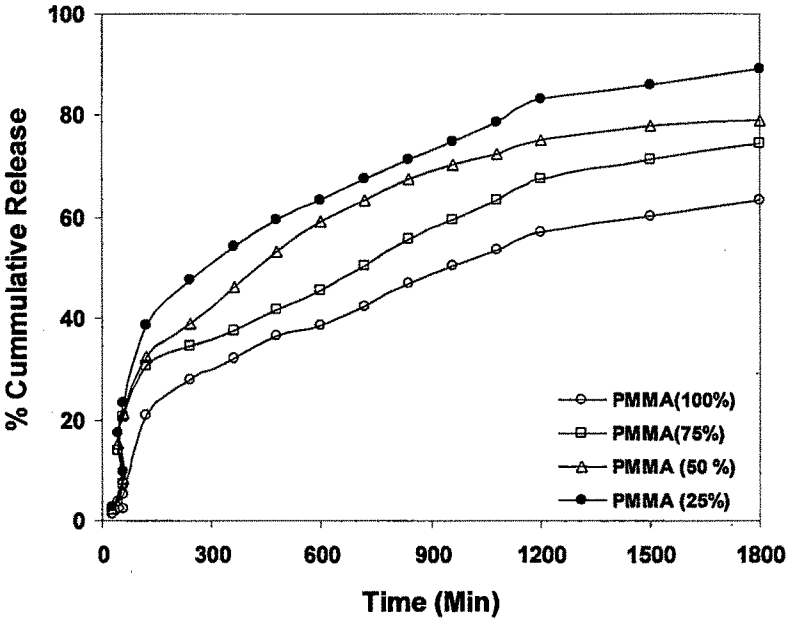

Figure 3.15 Percentage cumulative release pattern of etoposide through copolymeric nanoparticles. (•) PMMA, (Δ) (75:25) MMA-co-VCL, (□) (50:50) MMA-co-VCL, (O) 25:75 (MMA-co-VCL).

3.4.11 In-vitro cytotoxicity

As a part of our ongoing research in the development of novel CR systems attempts are made to synthesize various acrylate based nanoparticles for the entrapment of model drugs like acryflavin, carbamazepine and lamotrigine for the investigation of their release patterns through emulsion and microemulsion polymerization technique. Polymeric nanoparticles are being used for encapsulation of drugs, but very few attempts are made for biological applications of such systems. Polyacrylates nanoparticles are commonly used in biomedical applications, but toxicity associated with nanoparticles itself has not been systematically addressed. Likewise, evaluation of microcidal activity and cytotoxicity of surfactants, though thoroughly investigated, requires closer criticism in terms of their utilization in nanoparticles based drug delivery. Hoffman *et al*[87] synthesized methyl methacrylate based copolymeric nanoparticles by free radical polymerization and cytotoxicity of nanoparticles was determined in three different cell cultures including human foreskin fibroblast and two kidney cell lines MA-104 and Vero. They have reported IC_{50} values of nanoparticles in the range of 27.2-500 μg/mL for these cell lines. Similarly Turos *et al* [88-90] synthesized various polyacrylate based antibiotic formulations for life-theratening bacterial infections and cytotoxicity of nanoparticles emulsion was evaluated using human dermal fibroblast. They reported the importance of various purification processes and concluded that the formulations with more than 3 wt % of SDS remained cytotoxic to human keratinocytes even after purifications. However, the concentration of surfactant used in the synthesis of copolymeric nanoparticles plays an important role in stabilizing the final latex and controlling the particle size. It has been observed before that the toxicity of surfactants, including SDS in particular, depends on weather surfactant is unassociated (in bulk) or is bound to the surface of nanoparticles. This agrees with a prior report that SDS in aqueous medium is cytotoxic, but SDS associated with a matrix such as polymeric nanoparticles is not[91]. This led us to consider the possibility that any unassociated SDS present in the emulsion could perhaps be removed after the formation of nanoparticles, so as to decrease cytotoxic effect without changing the morphological features of the nanoparticle latex. Thus our focus was to remove SDS and other contaminanants (oligomers, nonstabilized polymers, along with residual unreacted monomers) from the microemulsion and to evaluate the nanoparticles emulsion for primary cell-

viability studies of B16F10 melanoma cell lines. Hence we have tried different purification routes in order to remove unassociated surfactant. Polymeric nanolatex was stored at 16 °C (Kraft temperature of SDS) for a period of week in order to remove all unassociated surfactant. The process was repeated till no further precipitation was observed. After that, polymeric nanolatex was further purified by ultra filtration unit (PALL, Mumbai, India) using omega membrane (OAD65C12), minimate tangential flow filtration capsule (MWCO 650 daltons) at room temperature (30 ± 2 °C). This step removes unassociated surfactant and other contaminanants such as oligomers, non stabilized polymers, along with residual unreacted monomers.

Further study on possible effects of the polymeric nanolatex on B16F10 melanoma cell lines, which is a decisive factor in weather these nanoparticles can be used for drug delivery system was undertaken. Thus, in-vitro cytotoxicity studies were conducted with the series of copolymeric nanoparticles against B16F10 melanoma cell lines.

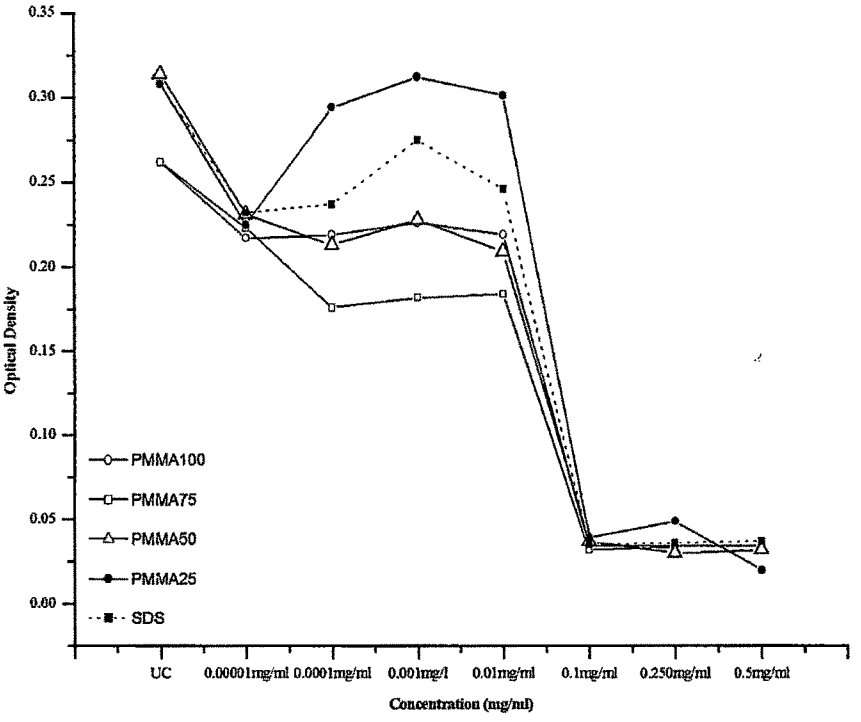

Figure 3.16 Cytotoxicity profiles of poly (MMA-co-VCL) nanoparticles of different compositions and SDS as a control, tested in B16F10 cell lines.

Figure 3.16 shows the cytotoxicity profiles of the different compositions of polymeric nanolatexes and control (SDS) at a concentration range 0.00001-0.5 mg/mL for 24 hrs. MTT-tests demonstrated that an increase in polymer concentration from 0.00001 mg/mL to 0.01 mg/mL was not harmful for the survival of cells at all compositions. Interestingly, it was observed from the preliminary data that, cytotoxicity of the nanoparticles decreases and cell-proliferation was observed with respect to VCL content of the copolymer in the concentration range under observation.

Simultaneously we have also tried to find out the cytotoxicity effect of model drug etoposide and etoposide entrapped copolymeric nanoparticles. In-vitro cytotoxicity effect of etoposide and etoposide loaded (MMA-co-VCL) nanoparticles on B16F10 cells were studied for a period of 24 hrs. ***Figure 3.17*** shows the cytotoxic effect of etoposide and etoposide loaded copolymeric nanoparticles on B16F10 melanoma for a period of 24 h. Etoposide, placebo nanoparticles and etoposide loaded nanoparticles inhibit B16F10 melonoma cell viability. The preliminary evaluation of cell-viability data shows that, IC_{50} value of etoposide and etoposide loaded polymeric nanoparticles was observed to be in the range of 0.00001-0.0001 mg/mL and 0.01-0.1 mg/mL respectively.

The synthesis of poly (MAA-co-VCL) nanoparticles loaded with etoposide in this study may lead to a new approach for delivery of etoposide and many other hydrophobic therapeutic agents. By utilizing this technique, high dose of etoposide can be initially injected and etoposide will be slowly released from the nanoparticles. Since etoposide will be released at a lower rate from nanoparticles, the nanoparticles minimize the systematical toxicity and reduce the number of administrations necessary to maintain systematic concentrations of etoposide. This type of system could also be utilized for local therapy if injected at the site of a tumor due to particle diameter which ranged from 20-50 nm. A thermo-responsive nature of polymer support may help the controlled release of etoposide at tumor site.

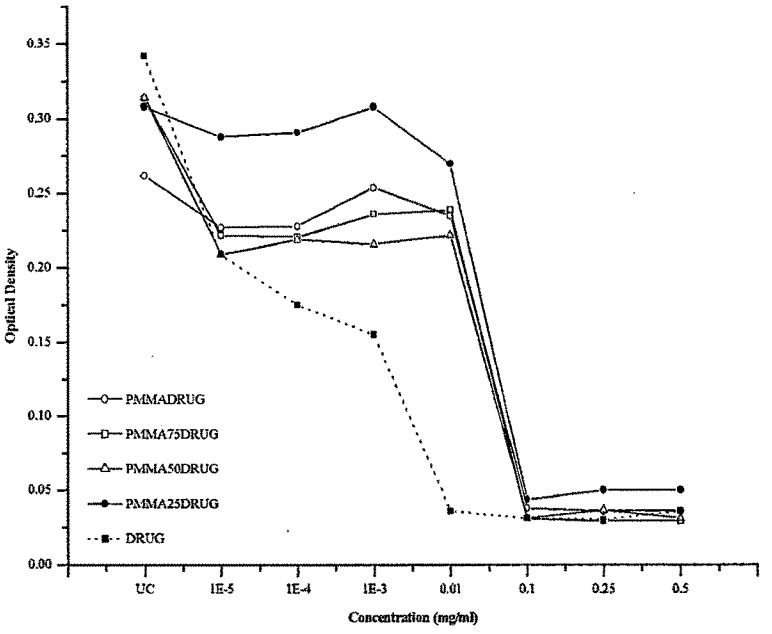

Figure 3.17 Cytotoxicity profiles of etoposide loaded poly (MMA-co-VCL) nanoparticles of different compositions and etoposide as a control, tested in B16F10 cell lines.

This preliminary biological characterization data indicates the possible technologically important route for etoposide based nanoparticles formulation and needs further research in this area.

3.4 Conclusion

Thermally responsive copolymeric nanolatex was synthesized through a continuous gradual feed micro emulsion polymerization technique. The copolymers produced by the gradual feed technique showed more homogeneous composition. Monomer reactivity ratios determined by Fineman-Ross, Inverted Fineman-Ross and Tidwell-Mortimer methods showed good correlation between the linear and nonlinear least square methods. It was observed that the studied monomer pair has a tendency to form random copolymer in the chosen monomer feed. TEM and DLS analysis of nanolatex confirmed the formation of well defined reasonably well mono-dispersed particles of size approximately in the range of 30 ± 5 nm with nearly spherical morphology for placebo and etoposide loaded nanoparticles and latex remained stable for a period of more than six months at room temperature. Cloud point temperature values of the copolymers were observed to vary with copolymer composition and copolymers with more than 40 % VCL content showed cloud temperature near to body temperature. Polyacrylate nanoparticles are commonly used in biomedical applications, but toxicity associated with nanoparticle forms has not been systematically determined. MTT-cytotoxicity tests demonstrated that an increase in polymer concentration from 0.00001 mg/mL to 0.01 mg/mL was not harmful for the cell survival in each composition

The addition of a model high molecular weight drug etoposide to polymeric nanoparticles, synthesized through micro emulsion polymerization proved to be successful with a 67-35 % drug entrapment with respect to copolymer compositions. The incorporation of etoposide did not appear to interfere significantly in the physicochemical properties of the polymer such as structure, molecular weight, particle size and morphology. IR and ^{1}H NMR analysis confirmed the copolymer formation. DSC and XRD analysis indicate the molecular level dispersion of drug in polymeric matrix. TEM, DLS and GPC analysis of nanolatex confirmed the formation of well defined reasonably well mono-dispersed particles with spherical morphology. As the VCL content increases in copolymer, increase in particle size and polydispersity and decrease in molecular weight and encapsulation efficiency of etoposide was observed. Release profile of etoposide from copolymeric nanoparticles shows initial burst effect followed by continuous slow release for a period of 30 hours

indicating a sign of controlled release of etoposide from nanoparticles. The preliminary evaluation of cell-viability data shows that, IC_{50} value of etoposide and etoposide loaded polymeric nanoparticles was observed to be in the range of 0.00001-0.0001 mg/ml and 0.01-0.1 mg/ml respectively. Overall, the technique indicates possible technologically important route for etoposide based nanoparticles formulation.

3.5 References

1. Park T.G., Hoffman A.S., *J. Appl. Polym. Sci.*,1992, **46,** 659.
2. Brazel C.S., Peppas N.A., *Mater. Res. Soc. Symp. Proc.*, 1994, **331,** 211.
3. Lim Y.H., Kim D., Lee D.S., *J. Appl. Polym. Sci.*, 1997, **64,** 2647.
4. Zhang J., Peppas N.A., *Macromolecules.*, 2000, **33,** 102.
5. Soppimath K.S., Aminabhavi T.M., Dave A.M., Kumbar S.G., Rudzinski W.E., *Drug Dev. Ind. Pham.*, 2002, **28,** 957.
6. Mahkam M., Allahverdipoor M., *J. Drug Targ.*, 2004, **12,** 151.
7. Zhang X., Wu D., Chu C.C., *Biomaterials.*, 2004, **25,** 4719.
8. Mardyani S., Chan W.C.W., Kumacheva E., *Adv. Mater.*, 2006, **18,** 80.
9. Soppimath K.S., Tan D.C.W., Yang Y., *Adv. Mater.*, 2005, **17,** 318.
10. Ballauff M., Lu Y., *Polymer.*, 2007, **48,** 1815.
11. Galaev I.Y., Gupta M.N., Mattiasson B., *Chem. Tech.*, 1996, **26,** 12.
12. Galaev I.Y., Mattiasson B., *Trends. Biotechnol.*, 2000, **17**, 335.
13. Murray M.J., Snowden M.J., *Adv. Colloid & Interface Sci.*, 1995, **54**, 73.
14. Jeong B., Gutowska A., *Trends. Biotech.*, 2002, **20,** 305.
15. Chen J.P., *J Chem. Tech. & Biotech.*, 1998, **73,** 137.
16. Rangarao K.V., Padmalatha K.D., *Int. J. Pharm.*, 1988, **48**, 1.
17. Okano T., Bae Y.H., Jacobs H., Kim S.W., *J. Control.Release.*,1990, **11,** 255.
18. Yoshida R., Sakai K., Ukano T., Sakurai Y., Bae Y.H., Kim S.W., *J. Biomat. Sci: Polym. Ed.*, 1991, **3,** 155.
19. Nujoma Y.N., Kim C.J., *J. Pharm. Sci.*,1996, **85,** 1091.
20. Lim Y.H., Kim D., Lee D.S., *J. Appl. Polym. Sci.*,1997, **64,** 2647.
21. Kikuchi A., Okano T. "*Biorelated Polymers and Gels: Controlled Release and applications in biomedical Engineering*", (Eds.), Okana T., Academic Press 1998, 1-28.
22. Hoffman A.S., *Adv. Drug Deliv. Rev.* 2002, **43,** 1.
23. Kopecek J., *Eur. J Pharm. Sci.*, 2003, **20**, 1.
24. Mahkam M., Allahverdipoor M., *J. Drug Targ.*, 2004, **12,** 151.
25. Freitag R., Baltes T., Eggert M., Schugerl K., Bahr U., *Bioseparation.*, 1994, **4,** 353.
26. Chen J. P., Jang F.L., *Biotech. Tech.*, 1995, **9,** 461.

27. Freitag R., Costioli M., Garret-Flaudy F., *Chimia.*, 2000, **55**, 196.
28. Costioli M.D., Fisch I., Garret-Flaudy F., Hilbrig F., Freitag R., *Biotech. & Bioeng.*, 2003, **81**, 535.
29. Hoffman A.S. "*Thermally reversible hydrogels containing biologically active species; Polymer in Medicine III*", (Ed.), Migliarese et al. Amsterdam, Elsevier Science Publishers B.V. 1988.
30. Chen J. P., *J. Chem. Tech. & Biotech.*, 1999, **73,** 137.
31. Ding Z., Chen G., Hoffman A.S., *J. Biomed. Mat. Res.*, 1998, **39,** 498.
32. Galaev I.Y., Mattiasson B., *Enz.& Microb. Tech.*, 1993, **15,** 354.
33. Ohya S., Nakayama Y., Matsuda T., *Biomacromolecules.*, 2001, **2**, 856.
34. Matsuda T., *Jap. J. Artif. Organs.*, 1999, **28,** 242.
35. Heskins M., Guilllet J.E., *J. Macromol. Sci. Chem.*, 1968, **55,** 1441.
36. Pelton R.H., Chibante P., *Colloids Surf.*, 1986, **20,** 247.
37. Kikuchi A., Okano T., *Prog. Polym. Sci.*, 2002, **27**, 1165.
38. Hoffman A.S., *J. Biomed. Mater. Res.*, 2000, **52**, 577.
39. Qui Y., Park K., *Adv. Drug Deliv. Rev.*, 2001, **53,** 321.
40. Chilkoti A., Dreher M.R., Meyer D.E. Raucher D., *Adv. Drug Deliv. Rev.*, 2002, **54,** 613.
41. Bromberg L.E., Ron E.S., *Adv. Drug Deliv. Rev.*, 1998, **31,** 197.
42. Weidner J., *Drug Discov. Today.*, 2001, **6,** 1239.
43. Sharma S., Kaur P., Jain A., Rajeswari M.R., Gupta M.N., *Biomacromolecules.*, 2003, **4,** 330.
44. Bignoti F., Penco M., Sartone L., Peroni I., Medichi R., Casolaro M., D'Amore A., *Polymer.*, 2000, **41**, 7.
45. Kurisawa M., Yui N., *J Control. Release.*, 1998, **54,** 191.
46. Diez-Pena E., Quijada-Garrido I., Barrales-Rienda J.M., *Polymer.*, 2002, **43,** 4341.
47. Varga I., Gilyani T., Meszaros R., Filipcsei G., Zrinyi M., *J. Phys. Chem. B.*, 2001, **105,** 9071.
48. Yoshida R., Uchida K., Kaneko Y., Sakai K., Kikuchi A., Sakurai Y., Okano T., *Nature.*, 1995, **374,** 240.
49. Jeong B., Lee K.M., Gutowska A., An Y.H., *Biomacromolecules.*, 2002, **3,** 865.
50. Hatifi A., Amsden B., *J Control. Release.*, 2002, **80,** 9.

51. Jeong B., Bae Y.H., Lee D.S., Kim S.W., *Nature.*, 1997, **388,** 860.
52. Chung J.E., Yokoyama M., Aoyagi T., Sakurai Y., Okano T., *J Control. Release.*, 1998, **53,** 119.
53. Nerdovic D., Van Nostrum C.F., Hennink W.E., *Macromoecules.*, 2001, **34,** 7589.
54. Stayton P.S., Shimoboji T., Long C., Chilkoti A., Chen G., Harris J.M., Hoffman A.S., *Nature.*, 1995, **378,** 472.
55. Leroux J., Roux E., Garrec D.L. Hong K., *J. Control. Release.*, 2001, **72,** 71.
56. Kirsh Y.E., *Water soluble poly-N-vinylamides.*, Chichester: Wiley; 1998.
57. Okhapkin I.M., Nasimova I.R., Makhaeva E.E., Khokhlov A.R., *Macromolecules.*, 2003, **36,** 8130.
58. Qiu X., Sukhishvili S.A., *J. Poly. Sci.: Part A; Polym. Chem.*, 2006, **11,** 163.
59. Ballauff M., Lu Y., *Polymer.*, 2007, **48**, 1815.
60. Mardyani S., Chan W.C.W., Kumacheva E., *Adv. Mater.*, 2006, **18**, 80.
61. Soppimath K.S., Tan D.CW., Yang Y., *Adv. Mater.*, 2005, **17**, 318.
62. Kawaguchi H., Fujimoto K., *Bioseperation.*, 1998, **4-5**, 253.
63. Sahiner N., Godbey W.T., Mcpherson G.L., John V.T., *Colloid & Polym. Sci.*, 2006, **284**, 1121.
64. Ivanov I.E., Kazakov S.V., Yu I., Mattiasson G.B., *Polymer.*, 2001, **42,** 3373.
65. Lowe T.L., Tenhu H., *Macromolecules.*, 1998, **31,** 1590.
66. Virtanen J., Baron C., Tenhu H., *Macromolecules.*, 2000, **33,** 336.
67. Laukkanen A., Hietala S., Maunu S.L., Tenhu H., *Macromolecules.*, 1998, **33,** 8703.
68. Laukkanen A., Weidmar S.K., Varjo S., Riekkola M.I., Tenhu H., *Colloid & Polym. Sci.*, 2002, **280,** 65.
69. Vihalo H., Laukkanen A., Hirovnen J., Tenhu H., *Eur. J. Pharm. Sci.*, 2002, **16,** 69.
70. Vihalo H., Laukkanen A., Valtola L., Tenhu H., Hirovnen J., *Biomaterials.*, 2005, **26,** 3055.
71. Galant C., Kjoniksen A.L., Kenneth D., Knudsen G.H., Laukkanen A., Tenhu H., Nystro B., *Langmuir.*, 2005, **21,** 8010.
72. Boutris C., Chatzi E.G., Kiparissides C., *Polymer.*, 1997, **38,** 2567.
73. Yan X., Gemeinhart R.A., *J. Control. Release.*, 2005, **106,** 198.
74. Yu E., Kirsh N.A., Yanul K., Kalninsh K., *Eur. Polym. J.*, 1999, **35,** 305.

75. Fineman M., Ross S.D., *J. Polym. Sci.*, 1950, **5,** 259.

76. Tidwell P.W., Mortimer G.A., *J. Poly. Sci.: Part A.*, 1965, **3,** 1369.

77. Yin and Stover., *Macromolécules.*, 2003, **36,** 9817.

78. Fujishige S., *Polymer J.*, 1987, **19,** 297.

79. Lessard D.G., Ousalem M., Zhu X. X., *Can. J. Chem.*, 2001, **79,** 1870.

80. Schild H.G., Tirrell D.A., *J. Phy. Chem.*, 1990, **94,** 4352.

81. Schild H.G., Tirrell D.A., *Langmuir.*, 1990, **6**, 1676.

82. Tong Z, Zeng F., Zheng X., Sato T., *Macromolecules.*, 1999, **32,** 4488.

83. Idziak I., Avoce D., Lessard D. Gravel D., Zhu X.X., Idziak I., *Macromolecules.*, 1999. **32**, 1260.

84. Jasti B.R., Du J., Vasavada R.C., *Int. J. Pharm.*, 1995, **118,** 161.

85. Babu Ramesh V., Malladi S., Hosamani K.M., Aminabhavi T.M., *Int. J. Pharm.*, 2006, **325,** 55.

86. Yao Z., Zhang C., Ping Q., Yu L., *Carbohydrate Polym.*, 2007, **68,** 781.

87. Hoffmann F., Cinatl Jr J., Kabickova H., Cinatl J., Kreuter J., Stieneker F., *Int. J Pharm.*, 1997, **157,** 189.

88. Garay-Jimenez J.C., Young A., Gergeres D., Greenhalgh K., Turos E., *Nanomedicine: NBM.*, 2008, **4,** 98.

89. Abeylath S.C., Turos E., *Carbohydrate Polym.*, 2007, **70**, 32.

90. Turos E., Shim J.Y., Wang Y., Greenhalgh K., Reddy S.G., Dickey S., Lim D.V., *Bioorg. Med. Chem. Lett.*, 2007, **17,** 53.

91. Muller R.H., Ruhl D., Runge S., Forster K.S., Mehnert W., *Pharma Research.*, 1997, **14,** 458.